

Numerical calculation of the Landauer conductance through an interacting electron system in the Hartree-Fock approximation

Yoichi A. Sada

Department of Physics, Tokyo Institute of Technology, 2-12-1 Ohokayama, Meguro-ku, Tokyo 152-8551, Japan

We develop a new numerical method to calculate the Landauer conductance through an interacting electron system in the first order perturbation or in the self-consistent Hartree-Fock approximation. It is applied to one and two dimensional systems with nearest-neighbor electron-electron interaction.

KEYWORDS: Landauer conductance, electron-electron interaction, Hartree-Fock approximation

1. Introduction

The interplay between disorder and electron-electron interaction in quantum electron transport phenomena is one of the most challenging problems. Although the non-interacting approximation successfully explains many aspects of experiments,¹ we may need to take into account the electron-electron interaction to understand some phenomena, such as the metallic behavior in two dimensional (2D) systems in Si-MOS and heterostructures,² and the critical phenomena of the 3D metal-insulator transitions.³ In theoretical works, important corrections due to electron-electron interaction in disordered electron systems were found.⁴⁻⁸ Furthermore, the study of the nonlinear model suggested new universality classes for the metal-insulator transition.⁹

The Hartree-Fock (HF) approximation was employed in some numerical works to study interacting disordered electron systems.¹⁰⁻¹⁸ It enables us to simulate relatively large systems. Even at the level of the HF approximation, however, our understanding is not yet complete. One of the reasons is the lack of numerical simulations of the Landauer conductance. As used in the scaling theory of Anderson localization¹⁹ (See Refs. 20-22 for more detailed discussions on the scaling hypothesis of the Landauer conductance.), the conductance is one of the most important physical quantities to characterize a disordered electron system. We expect that numerical simulation of the Landauer conductance would improve our understanding on the interplay between disorder and electron-electron interaction.

Motivated by this, we have decided to perform a numerical calculation of the Landauer conductance in interacting disordered electron systems in the HF approximation. As a first step toward it we have developed a numerical method, which we report here.

The generalization of the Landauer approach to interacting electron systems is a very active topic not only to study interacting disordered electron systems but also to study transport phenomena through low dimensional electron systems. Although much progress has been made in the generalization of the Landauer approach,²³⁻³⁶ the calculation method is still being improved.

This paper is organized as follows: In §2 the model considered is described and in §3 the Landauer formula

is described. The HF approximation is described in §4. In §5, we explain a new numerical method, which we call wide band method. In §6 and §7, we apply the wide band method to 1D and 2D systems of interacting electrons. The last section is devoted to summary and discussion.

2. Model

We consider spinless electrons on a 2D square lattice. As illustrated in Fig. 1, the system considered consists of a sample region with size $L_x \times L_y$ (denoted by S) and two semi-infinite leads with width L_y (denoted by L). We impose fixed boundary conditions in the transverse direction. We suppose that electrons are interacting in the sample region, while non-interacting in the lead region. In the present paper we do not consider random potential for simplicity. We take the x direction as the current direction and y direction as the transverse direction.

The tight binding Hamiltonian is given by

$$H = H_s + H_\ell + H_r + H_u; \quad (1)$$

where H_s is the non-interacting part for the sample region S , H_ℓ the Hamiltonian for the perfect leads at the left and right, H_r the coupling between the sample and leads, and H_u electron-electron interaction in the sample region. They are given by

$$H_s = \sum_{i,j \in S} t_{ij} c_i^\dagger c_j; \quad (2)$$

$$H_\ell = \sum_{i,j \in L} t_{ij} c_i^\dagger c_j; \quad (3)$$

$$H_r = \sum_{y=1}^{L_y} t_{0,y} c_{0,y}^\dagger c_{1,y} + c_{1,y}^\dagger c_{0,y} + \sum_{y=1}^{L_y} t_{L,y} c_{L,y}^\dagger c_{L+1,y} + c_{L+1,y}^\dagger c_{L,y}; \quad (4)$$

$$H_u = \frac{1}{2} \sum_{i,j \in S} c_i^\dagger c_i K_{U_{ij}} c_j^\dagger c_j K_{ij}; \quad (5)$$

Here c_i^\dagger (c_i) denotes the creation (annihilation) operator of an electron at the site i , U_{ij} is the interaction between

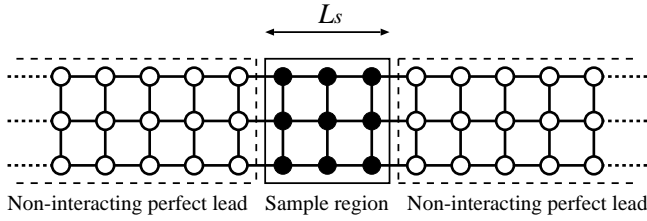


Fig. 1. An example of the Landauer geometry to calculate the two-terminal conductance. Two non-interacting perfect leads are attached to the sample.

electrons at the sites i and j , and K is a positive uniform charge. Hopping is restricted to nearest-neighbors. We suppose that the hopping parameters t_s , t_l , and t_s are real, so the system has time reversal symmetry.

3. Landauer conductance

The Landauer conductance g at zero temperature in the linear response regime is expressed using Green's functions as

$$g = \frac{e^2}{h} \text{tr} \left(G_{1L_s}^a(\mu) G_{L_s 1}^r(\mu) \right) \quad (6)$$

Here μ is the chemical potential of the system, $G_{L_s 1}^r$ and $G_{1L_s}^a$ the submatrices of the retarded and advanced Green's functions in equilibrium, and $G_{L_s 1}^{(L;R)}$ the matrices determined by the attached leads.²³ The matrices $G_{L_s 1}^{(L;R)}$ are explicitly shown in Appendix .

It has been shown in Refs. 29 and 31 that the expression (6), which is well known for non-interacting electrons,²³ is valid even when electrons are interacting in the sample region at zero temperature. Within the HF approximation the expression (6) can also be justified based on the Keldysh Green's function method.²³

In the following sections, we only consider the retarded Green's function G^r since the advanced Green's function G^a is simply Hermitian conjugate of the retarded Green's function.

4. Hartree-Fock approximation

We describe the HF approximation in the Green's function formalism³⁷ for the system (1).

The Dyson equation for G^r in the HF approximation is obtained by expanding the time-ordered Green's function in H_U and by performing an analytic continuation. We have

$$G^r(\omega) = G_0^r(\omega) + G_0^r(\omega) ({}^{HF}) G^r(\omega) \quad (7)$$

Here G_0^r is the retarded Green's function for the non-interacting part of the Hamiltonian $H_0 = H_s + H_l + H_{ls}$, and $({}^{HF})$ is the self-energy due to electron-electron interaction in the HF approximation, which is non-zero only in the sample region. It consists of Hartree and exchange contributions:

$$({}^{HF})_{ij;i} = \sum_{j(j \neq i)}^X U_{ijj} \frac{1}{\omega} \int_1^Z d \text{Im} G_{jj}^r(\omega) K \quad ; \quad (8)$$

$$({}^{HF})_{ij;j(i \neq j)} = \frac{U_{ijj}}{\omega} \int_1^Z d \text{Im} G_{ijj}^r(\omega) \quad ; \quad (9)$$

where $i, j \in S$. (In more general expression, $\text{Im} G^r(\omega)$ is replaced with $(\omega \mp 2) [G^r(\omega) - G^a(\omega)]$. For our model, they are the same.) From (7), we have

$$G^r(\omega) = \frac{h}{H_0 - (\omega - i\epsilon) + ({}^{HF})} \quad ; \quad (10)$$

Here H_0 is the single particle Hamiltonian in the matrix form corresponding to the non-interacting part H_0 and ϵ is an infinitesimal positive number. The HF self-energy $({}^{HF})$ is a solution of the self-consistent equations (8)–(10).

In practice there are two difficulties we need to solve:

Since the Landauer geometry corresponds to an open system, the size of the matrix H_0 is infinite. We need to make the matrix size finite to perform numerical simulations.

To calculate the HF self-energy $({}^{HF})$, we need to perform an integral over ω .

The first problem can be solved by taking account of the effects of the semi-infinite leads in terms of a self-energy.^{23,38(40)} For example, if we expand the Green's function in H_{ls} in addition to H_U , we obtain the Dyson equation for the retarded Green's function G_{ijj}^r ($i, j \in S$) in the HF approximation in a finite size matrix form that is closed in the sample region S . The Green's function G_{ijj}^r , with $i, j \in S$, is written as

$$G^r(\omega) = \frac{h}{H_s - (\omega - i\epsilon) + ({}^{HF}) + ({}^{lr})} \quad ; \quad (11)$$

Here H_s is the single particle Hamiltonian in the matrix form corresponding to H_s , $({}^{HF})$ is the HF self-energy which is given by Eqs. (8) and (9), and $({}^{lr})$ is the retarded self-energy due to the attached semi-infinite leads. An element of the self-energy $({}^{lr})_{xy;xy^0}$ is non-zero only when $x = x^0 = 1$ or $x = x^0 = L_s$. The non-zero elements are written as (see Appendix)

$$({}^{lr})_{xy;xy^0}(\omega) = \frac{t_s^2}{t_l} \sum_n^X \frac{X}{t_l} \frac{v_n(\omega) v_n(\omega^0)}{t_l} \quad ; \quad (12)$$

where $X = 1$ or L_s . The Green's function G_{ijj}^r ($i, j \in S$) of (11) is exactly the same as that of (10) since we have taken into account all orders in H_{ls} . Now in (11) the size of the matrices is finite, $L_s L_y \times L_s L_y$, so it is possible to perform numerical calculations in principle.

As for the second problem, a numerical integration was employed in similar approaches.^{39,40} The numerical integration of the Green's function is not very difficult if a simple system is considered. However the numerical integration is troublesome in general, so we have developed a method to avoid it. The method is explained in the next section.

5. Wide band method

We have developed a new method, which we call wide band method, to avoid the numerical integration as follows.

We change the system considered from the original Landauer system, illustrated in Fig. 1, to another system as illustrated in Fig. 2. We call it wide band system. The lead region is divided into two parts: the region C up to

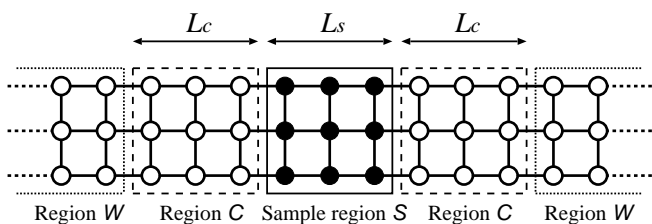


Fig. 2. The system envisaged in the wide band method. Each non-interacting lead is divided into two regions C and W.

a length L_c on both sides of the sample, and the region W consisting of two semi-infinite regions. The wide band system is described by the following Hamiltonian,

$$H = H_s + H' + H_{vs} + H_u; \quad (13)$$

Here H_s, H_{vs} , and H_u are already given in (2), (4), and (5). The other term H' for the leads is made of three terms

$$H' = H_c + H_w + H_{cw}; \quad (14)$$

which are given by

$$H_c = \sum_{i,j \in C} t_{ij} c_i^\dagger c_j; \quad (15)$$

$$H_w = \sum_{i \in W} t_w c_i^\dagger c_i + \sum_{i,j \in W} t_{ij} c_i^\dagger c_j; \quad (16)$$

$$H_{cw} = \sum_y t_{cw} c_{X_L}^\dagger c_{X_L+1,y} + \sum_y c_{X_L,y}^\dagger c_{X_L-1,y} + \sum_y c_{X_R,y}^\dagger c_{X_R+1,y} + \sum_y c_{X_R+1,y}^\dagger c_{X_R,y}; \quad (17)$$

with $X_L = L_c + 1$ and $X_R = L_s + L_c$. Here H_c is the Hamiltonian for the finite regions C on the sample, H_w the Hamiltonian for the semi-infinite regions W, and H_{cw} the coupling between the regions C and W. Two hopping parameters t_w, t_{cw} and one parameter for uniform potential w are introduced for the wide band system. If $t_w = t_{cw} = t$ and $w = 0$, the Hamiltonian (13) is exactly the same as the original Hamiltonian (1), which is the system we want to solve. However, as we explain below, we take a limit $t_w, t_{cw}; w \rightarrow 1$ under certain conditions (conditions (24) and (25)). We call this limit wide band limit since the band width in the region W becomes infinity in the limit $t \rightarrow 1$.

We expand the Green's functions in H_{cw} and H_u . The retarded Green's function for the wide band system (13) in the HF approximation is written as,

$$G^r(\omega) = \frac{1}{H_t - \tilde{\Sigma}^{(HF)}(\omega) - i0^+}; \quad (18)$$

Here H_t is the Hamiltonian in a matrix form corresponding to $H_t = H_s + H_{vs} + H_c$, $\tilde{\Sigma}^{(HF)}$ the selfenergy in the HF approximation for the system (13)

$$\tilde{\Sigma}_{ij}^{(HF)} = \sum_{j \in C} U_{ij} \frac{1}{\omega} \int_0^Z d\text{Im} G_{jj}^r(\omega) K; \quad (19)$$

$$\tilde{\Sigma}_{ij}^{(HF)} = \frac{U_{ij}}{\omega} \int_0^Z d\text{Im} G_{ij}^r(\omega); \quad (20)$$

where $i, j \in C$, and $\tilde{\Sigma}^{(w)r}$ the retarded selfenergy due to the semi-infinite region W. An element $\tilde{\Sigma}_{xy;x'y^0}^{(w)r}$ is non-zero only when $x = x^0 = X_L$ or $x = x^0 = X_R$. The non-zero elements are given by

$$\tilde{\Sigma}_{xy;x'y^0}^{(w)r} = \frac{t_{cw}^2}{t_w} X_n(\omega) X_n(\omega^0) \frac{w}{t_w} \delta_{xy}; \quad (21)$$

where $X = X_L$ or X_R . The size of matrices in (18) is finite, $(L_s + 2L_c)L_y \times (L_s + 2L_c)L_y$. We use the tilde to denote that they are the Green's function and the self-energy not for the original system but for the wide band system.

In the semi-infinite regions W we take the wide band limit. In this limit the selfenergy $\tilde{\Sigma}^{(w)r}$ becomes independent of ω and the non-zero elements of $\tilde{\Sigma}^{(w)r}$ are equal to

$$\tilde{\Sigma}_{xy;x'y^0}^{(w)r} = t_w \frac{X_n(\omega) X_n(\omega^0)}{t_w} \delta_{xy}; \quad (22)$$

This limit is obtained by taking the limit,

$$t_w, t_{cw}; w \rightarrow 1; \quad (23)$$

while keeping

$$t_{cw}^2 = t_w = t; \quad (24)$$

$$w = t_w = t; \quad (25)$$

(When $w = 0$, we do not need to introduce w .)

A similar idea to use an energy independent self-energy can be seen in many papers, for example, Refs. 31 and 41. Two important differences from previous works are:

We keep non-interacting regions up to a length L_c on both sides of the sample to reduce artifacts of taking the wide band limit.

The selfenergy for the wide band region is chosen so that electrons at $\omega = \epsilon_F$ are not scattered at the boundaries between C and W. This makes it easier to reduce the artifacts.

The selfenergy (22) in the wide band limit is equal to the selfenergy at $\omega = \epsilon_F$ for the original system, i.e., the selfenergy (21) with $t_w = t_{cw} = t$ and $w = 0$. This means that electrons at the Fermi energy ϵ_F are not scattered at the boundaries between the regions C and W. When electron-electron interaction is neglected, the Landauer conductance for the wide band system is exactly the same as that for the original Landauer system since the selfenergy only at $\omega = \epsilon_F$ is relevant for the conductance in non-interacting systems. When we take account of the electron-electron interaction, the conductances for the wide band system and for the original system are no longer the same, because electrons below the Fermi energy affect the motion of electrons at the Fermi energy through the HF self-energy. To reduce such artifacts of taking the wide band limit on the calculated conductance, we keep non-interacting regions up to a length L_c on both sides of the sample. We expect that the artifacts of taking the wide band limit decrease as L_c increases, and they are finally removed in the limit $L_c \rightarrow \infty$.

The absence of boundary scattering for electrons at $\epsilon = \epsilon_c$ is important for the efficiency in removing the artifacts. If electrons near $\epsilon = \epsilon_c$ are scattered strongly at the two boundaries, resonant states due to the boundary scattering can be formed near $\epsilon = \epsilon_c$. In this case, the Green's function $G^r(\epsilon)$ at the Fermi energy shows larger fluctuation as a function of L_c , and we need to simulate systems with longer L_c to remove the artifacts. On the other hand, our choice to minimize the boundary scattering of electrons near the Fermi energy, that makes it easier to reduce the artifacts of taking the wide band limit.

By taking the wide band limit, the self-energy $\tilde{\Sigma}^{(w)r}$ becomes independent of L_c . We define an effective Hamiltonian by

$$H^{(e)r} = H_t + \tilde{\Sigma}^{(w)r} + \tilde{\Sigma}^{(HF)}; \quad (26)$$

Then the Green's function (18) is written as

$$G^r(\epsilon) = \frac{h}{H^{(e)r} + i\epsilon} \quad (27)$$

Note that $H^{(e)r}$ is not a Hermitian matrix but is a complex symmetric matrix since H_t and $\tilde{\Sigma}^{(HF)}$ are real symmetric matrices and $\tilde{\Sigma}^{(w)r}$ is a complex symmetric matrix. The effective Hamiltonian has right and left eigenvectors

$$H^{(e)r} \mathbf{j}_n^i = q_n \mathbf{j}_n^i; \quad (28)$$

$$h_n^j \mathbf{j}^{(e)r} = h_n^j \mathbf{j}_n^j; \quad (29)$$

Here q_n is an eigenvalue, which is complex in general. Since the effective Hamiltonian is a complex symmetric matrix, the transpose of the corresponding right eigenvector is the left eigenvector,

$$h_n^j = \mathbf{j}_n^j{}^\dagger; \quad (30)$$

For convenience, we impose the following normalization conditions.

$$h_n^j \mathbf{j}_m^i = \delta_{nm}; \quad (31)$$

Then they satisfy the completeness relation,

$$\sum_n \mathbf{j}_n^i h_n^j = 1; \quad (32)$$

By using eigenvalues q_n and right eigenvectors \mathbf{j}_n^i , the retarded Green's function is expressed as^{23,42}

$$G_{i,j}^r(\epsilon) = \sum_n \frac{\mathbf{j}_n^i \mathbf{j}_n^j}{q_n + i\epsilon}; \quad (33)$$

Here a_n and (b_n) are the real part and the imaginary part of the eigenvalue, $q_n = a_n - ib_n$, and $\mathbf{j}_n^i(j) = h_j \mathbf{j}_n^i$.

To calculate the self-energy $\tilde{\Sigma}^{(HF)}$, we need to perform the integral of the imaginary part of the retarded Green's function

$$J_{i,j}(\epsilon; \epsilon_c) = \int_0^{\epsilon_c} d\epsilon \text{Im} G_{i,j}^r(\epsilon); \quad (34)$$

For a moment, we introduce a cutoff parameter ϵ_c . We will take the limit $\epsilon_c \rightarrow 1$ later. By using the expression

(33), the integral (34) can be performed analytically as

$$J_{i,j}(\epsilon; \epsilon_c) = \sum_n \left(\text{Re}[\mathbf{j}_n^i \mathbf{j}_n^j] [\mathbf{j}_n^i(\epsilon) \mathbf{j}_n^j(\epsilon_c)] + \text{Im}[\mathbf{j}_n^i \mathbf{j}_n^j] \ln \frac{\cos \mathbf{j}_n^i(\epsilon)}{\cos \mathbf{j}_n^i(\epsilon_c)} \right); \quad (35)$$

where $\mathbf{j}_n^i(\epsilon) = \tan^{-1} \frac{a_n}{b_n + \epsilon}$ is defined by

$$\mathbf{j}_n^i(\epsilon) = \tan^{-1} \frac{a_n}{b_n + \epsilon}; \quad (36)$$

For the second term in (35), we should not take the limit $\epsilon_c \rightarrow 1$ before taking the summation over n because of the logarithmic divergence

$$\ln[\cos \mathbf{j}_n^i(\epsilon_c)] = \ln \epsilon_c + \ln(b_n + \epsilon_c) + O(\epsilon_c^{-1}); \quad (37)$$

The logarithmic divergence disappears when we take the summation over n because (32) implies

$$\sum_n \text{Im}[\mathbf{j}_n^i \mathbf{j}_n^j] = 0; \quad (38)$$

Therefore, in the limit $\epsilon_c \rightarrow 1$ we have

$$J_{i,j}(\epsilon; 1) = \sum_n \left(\text{Re}[\mathbf{j}_n^i \mathbf{j}_n^j] \mathbf{j}_n^i(\epsilon) + \frac{i}{2} + \text{Im}[\mathbf{j}_n^i \mathbf{j}_n^j] \ln \frac{\cos \mathbf{j}_n^i(\epsilon)}{b_n + \epsilon} \right); \quad (39)$$

Thus we calculate the self-energy from the eigenvalues and the right eigenvectors of $H^{(e)}$ without performing numerical integration.

Finally the numerical implementation of the wide band method is summarized. First we prepare an initial matrix for $\tilde{\Sigma}^{(HF)}$. Then we calculate the eigenvalues and eigenvectors by diagonalizing the effective Hamiltonian $H^{(e)r}$. From the eigenvalues and right eigenvectors, we calculate the self-energy $\tilde{\Sigma}^{(HF)}$, (19) and (20), by using (39). We continue this self-consistent iteration until $\tilde{\Sigma}^{(HF)}$ converges with enough precision. (To ensure convergence, we have used the method of potential mixing¹⁷) After convergence, we calculate the conductance $\mathcal{G}(L_c)$ for the wide band system by using the expression (6), where $G^{r;s}(\epsilon)$ is substituted for $G^{r;s}(\epsilon)$. We expect that the conductance $\mathcal{G}(L_c)$ for the wide band system approaches to the conductance g for the original system in the limit $L_c \rightarrow 1$,

$$g = \lim_{L_c \rightarrow 1} \mathcal{G}(L_c); \quad (40)$$

In the case of 1D system (x6) we extrapolate $\mathcal{G}(L_c)$ by using an empirical fitting function. In the case of 2D system (x7) we make L_c large enough so that the artifacts of the wide band limit can be negligible to a good approximation.

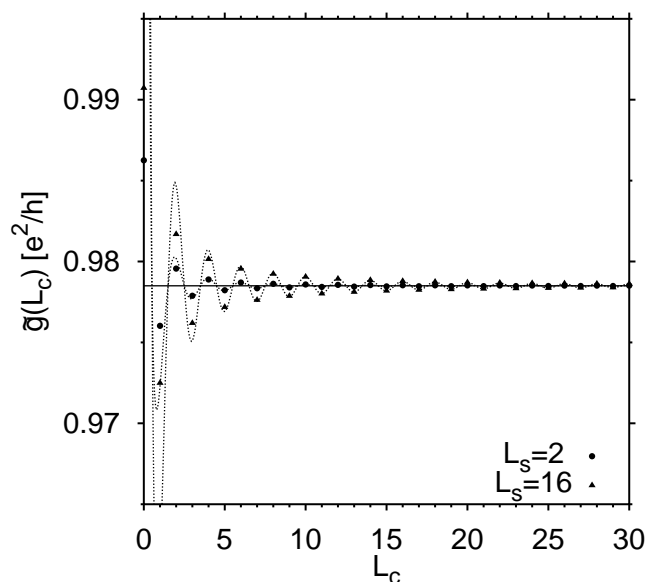


Fig. 3. The conductance $g(L_c)$ for the wide band system calculated with the wide band method in 1D in the first order perturbation is shown as a function of L_c . We set $K = 0.5$, $\mu = 0.0$, and $U = 0.5$. The dotted lines are the fit of (45) to the data with $L_c = [1; 30]$. The fit deviates from the numerical data when L_c is much smaller than this range. The solid line indicates the conductance for the original system, $g = 0.9785e^2/h$, obtained from (44).

6. Application to a 1D system

6.1 System

Here we calculate the Landauer conductance in a 1D system, i.e. $L_y = 1$, described by the Hamiltonian (1). We suppose that the hopping parameter is uniform in the system and set it unity as a unit of energy, $t_s = t_x = t_y = 1$. We also suppose that two electrons are interacting only when they occupy the nearest neighbor sites,

$$U_{x;x^0} = \begin{cases} U & (\text{if } x^0 = x - 1) \\ 0 & (\text{otherwise}): \end{cases} \quad (41)$$

Transport phenomena in this model was previously studied in Refs. 34{36,43. We set the positive background charge $K = 0.5$ and the Fermi energy $\mu = 0$, which corresponds to half-filling. Since we use the first order perturbation or the self-consistent HF approximation the electron-electron interaction should be weak, so we set $U = 0.5$.

6.2 In the first order perturbation

First we calculate the Landauer conductance in the first order perturbation to test the wide band method. Since the system studied here is very simple, the conductance in the first order perturbation for the original Landauer system (1) can be calculated analytically without making use of the wide band method. By comparing the numerical results of the wide band method with the analytical results, we test the wide band method.

The self-energy in the first order perturbation for the original system (1) is obtained by replacing G^r in (8) and (9) with the Green's function G_0^r for the non-interacting

Hamiltonian H_0 . The first order Hartree term is zero because the uniform negative charge of the electrons cancels with the uniform positive charge in the background. The first order exchange term at $\mu = 0$ is given by

$$\Sigma_{x;x+1}^{(1st)} = \frac{U}{h} (1 - x - L_s - 1): \quad (42)$$

From this self-energy, we obtain the conductance in the first order perturbation. When L_s is odd, we have a perfect transmission,

$$g = \frac{e^2}{h} \quad (L_s : \text{odd}): \quad (43)$$

For even L_s we have

$$g = \frac{e^2}{h} \frac{2(1 + U =)^2}{(1 + U =)^2 + 1} \quad (L_s : \text{even}): \quad (44)$$

When $U = 0.5$ and L_s is even, we find $g' = 0.9785e^2/h$.

We have also calculated the conductance in the first order perturbation by using the wide band method. The numerical result in the first order perturbation has been obtained by stopping the self-consistent iteration after just one iteration. When L_s is odd, the conductance is always e^2/h independent of L_c and L_s . When L_s is even, the conductance is reduced from e^2/h . As shown in Fig. 3, $g(L_c)$ oscillates as a function of L_c when L_s is even.

To remove the artifacts of taking the wide band limit, we need to extrapolate the conductance $g(L_c)$ to $L_c \rightarrow 1$. The extrapolation has been done by using an empirical fitting function of the form,

$$g(L_c) = g + a \frac{\cos(L_c)}{L_c^y}: \quad (45)$$

Here g , a , and y are fitting parameters. We expect that the asymptotic value g is equal to the conductance for the original system. By fitting numerical data with $L_c = [1; 30]$, we have found $g = 0.9785e^2/h$ for any even L_s in the range $L_s = [2; 16]$. The estimates of a and y weakly depend on the range of L_c used for the fit. On the other hand, the estimate of the asymptotic value g is stable against the change of the range of L_c .

The asymptotic value $g = 0.9785e^2/h$ for even L_s estimated with the wide band method is in good agreement with the analytical result (44) for the original Landauer geometry. The difference of the conductance is of order 10^{-8} to 10^{-6} in units of e^2/h . The good agreement indicates that the wide band method works well to estimate the conductance g by extrapolating the conductance $g(L_c)$ for the wide band system to $L_c \rightarrow 1$.

6.3 In the self-consistent Hartree-Fock approximation

We have then calculated the conductance in 1D in the HF approximation with the wide band method. When L_s is odd, we have found $g(L_c) = e^2/h$ for any L_c . When L_s is even, the conductance is reduced from e^2/h . We extrapolated the conductance for each even L_s to $L_c \rightarrow 1$ by using the fitting function (45), as in the case of the first order perturbation. Some numerical data and the corresponding fits are shown in Fig. 4. From the fit, we have obtained the asymptotic value g for each even L_s .

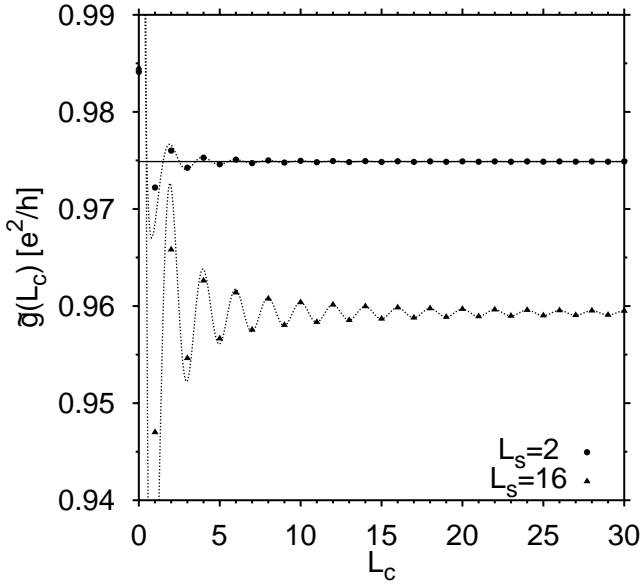


Fig. 4. The conductance $g(L_c)$ for the wide band system calculated with the wide band method in 1D in the HF approximation is shown as a function of L_c . We set $K = 0.5$, $\mu = 0.0$, and $U = 0.5$. The dotted lines are the fit of (45) to the data with $L_c = [1; 30]$. The fit deviates from the numerical data when L_c is much smaller than this range. The solid line indicates the conductance for the original system with $L_s = 2$, $g = 0.9749e^2/h$, obtained from (46) and (47). There is no solid line for $L_s = 16$ since it is too difficult for us to calculate the conductance for the original system with $L_s = 16$ in the HF approximation.

Even in the HF approximation it is not impossible to calculate the conductance g for the original system without using the wide band method. So far we have calculated g only for $L_s = 2$. The Hartree term $\Sigma_{x;x}^{(HF)}$ is zero when $\mu = 0$ because of the particle-hole symmetry. The exchange self-energy $\Sigma_{1;2}^{(HF)}$ for $L_s = 2$ is a solution of⁴⁴

$$1 - v = U \frac{v^2}{2v^2 - 1} \frac{1}{1 - \tan^{-1} \frac{2v}{v^2 - 1}} + \frac{1}{v}; \quad (46)$$

with $v = 1 \frac{\Sigma_{1;2}^{(HF)}}{v}$. From this equation we find $\Sigma_{1;2}^{(HF)} = 0.1733$ for $U = 0.5$. By using a formula for the conductance

$$g = \frac{e^2}{h} \frac{2(1 - \Sigma_{1;2}^{(HF)})^2}{(1 - \Sigma_{1;2}^{(HF)})^2 + 1}; \quad (47)$$

we find $g = 0.9749e^2/h$ for $L_s = 2$ and $U = 0.5$. This value of the conductance is indicated with a solid line in Fig. 4. The difference between this value and that estimated with the wide band method is of order $10^{-8}e^2/h$, indicating that the wide band method works well.

6.4 Length dependence of the conductance { comparison of numerical results

Figure 5 shows the L_s dependence of the conductance within the first order perturbation and within the HF approximation. For a reference, the conductance calculated with the embedding method by R. A. Molina and J.-L. Pichard⁴⁵ is also shown. In the embedding method, the electron-electron interaction is treated exactly, hence it is thought that the calculated conductance is also exact.

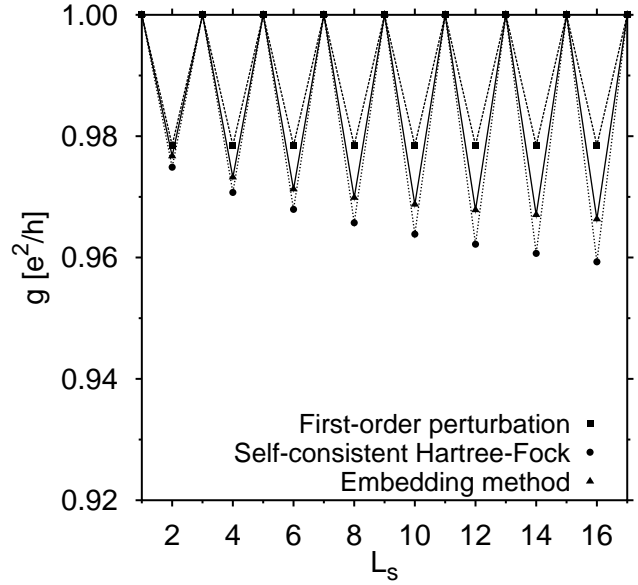


Fig. 5. L_s dependent oscillation of the conductance g in 1D. The conductance g in the first order perturbation and in the HF approximation are shown as well as that of the embedding method.⁴³ We set $K = 0.5$, $\mu = 0.0$, and $U = 0.5$. The data calculated by the embedding method were provided by R. A. Molina and J.-L. Pichard.⁴⁵ The lines are a guide to the eye only.

In all three cases, the perfect conductance $g = e^2/h$ is obtained when L_s is odd, and the conductance is reduced from it when L_s is even. This even-odd oscillation was found in Ref. 43. A similar parity oscillation in the Hubbard chain was reported in Ref. 30.

Within the first order perturbation, the conductance is independent of L_s for all even L_s . However, the result of the embedding method, which is thought to be exact, indicates that the conductance for even L_s decreases when L_s increases. The conductance for even L_s in the HF approximation also shows that the conductance decreases with increasing L_s . So we find a qualitative agreement between the behavior of the conductance in the HF approximation and that of the embedding method. Furthermore, the results indicate that the HF approximation is more accurate than the first order perturbation quantitatively.

7. Application to a 2D system

7.1 System

The application of the wide band method is not restricted to 1D systems. Here we apply it to a 2D system, i.e., a square system ($L_s = L_y$). The hopping parameter is supposed to be uniform and set it unity as a unit of energy, $t_x = t_y = t_s = 1$. We consider the nearest neighbor electron-electron interaction in the sample region,

$$U_{i;j} = \begin{cases} U & \text{(if } (i;j) \text{ is a nn pair)} \\ 0 & \text{(otherwise):} \end{cases} \quad (48)$$

In our simulation, we set the strength of electron-electron interaction $U = 0.5$. We set the chemical potential $\mu = 0$ and the positive charge $K = 0.5$, which corresponds to half-filling.

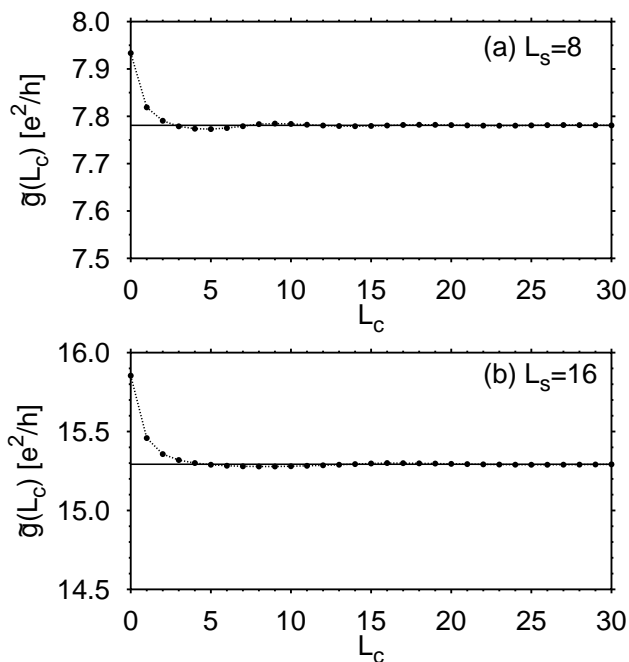


Fig. 6. The conductance $g(L_c)$ for the wide band system calculated with the wide band method in 2D in the first order perturbation for (a) $L_s = 8$ and (b) $L_s = 16$ is shown as a function of L_c . We set $K = 0.5$, $\mu = 0.0$, and $U = 0.5$. The dotted lines are a guide to the eye only. The solid lines indicate the conductance g for the original system obtained from (49) and (50) without using the wide band method.

7.2 In the first order perturbation

First we have calculated the conductance within the first order perturbation to test the wide band method in 2D as it has been tested in 1D in x6.

Within the first order perturbation, we can calculate the conductance without using the wide band method since the self-energy (1st) in the first order perturbation for the original Landauer system is obtained as follows. The Hartree contribution is zero since the positive background charge compensates the negative charge of electrons. The exchange contribution is given by

$$\chi_{xy}^{(1st)} = \frac{2U}{(L_y + 1)} \sum_{n=1}^{L_s} \sin k_y^{(n)} \sin^2 k_y^{(n)} y ; \quad (49)$$

$$\chi_{xy}^{(1st)} = \frac{2U}{(L_y + 1)} \sum_{n=1}^{L_s} k_y^{(n)} \sin k_y^{(n)} y \frac{i}{\sin k_y^{(n)} (y + 1)} ; \quad (50)$$

where $k_y^{(n)} = n/(L_s + 1)$. We have calculated (1st) by taking the summation over n in (49) and (50) numerically, and then have calculated the corresponding conductance g .

We have also calculated the conductance making use of the wide band method in the first order perturbation. Figure 6 shows the L_c dependence of the conductance $g(L_c)$ for the wide band system with sample size $L_s = 8$ and $L_s = 16$. For a reference, the conductance g calculated from (49) and (50) is also shown with the solid

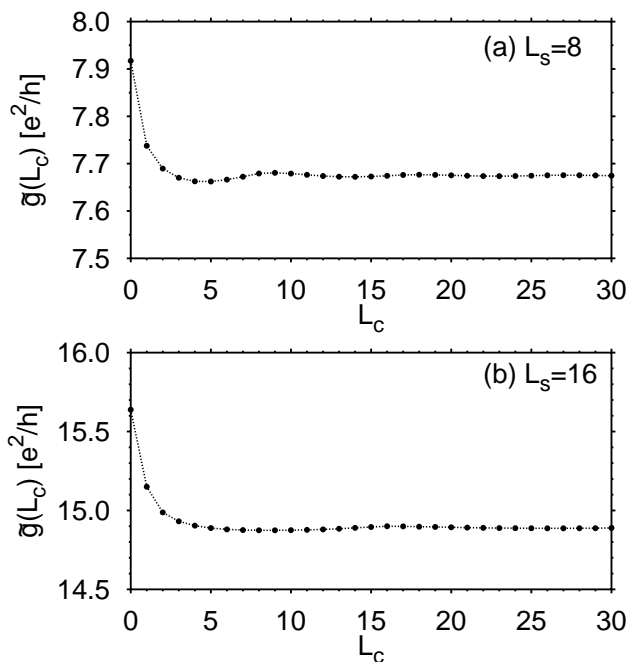


Fig. 7. The conductance $g(L_c)$ for the wide band system calculated with the wide band method in 2D in the HF approximation for (a) $L_s = 8$ and (b) $L_s = 16$ is shown as a function of L_c . We set $K = 0.5$, $\mu = 0.0$, and $U = 0.5$. The dotted lines are a guide to the eye only.

line. The figure indicates that $g(L_c)$ fluctuates around the value g and the fluctuation becomes smaller when L_c increases. It is reasonable to assume that the influence of the wide band limit is, to a good approximation, negligible when $L_c = 30$,

$$g \approx g(L_c = 30); \quad (51)$$

We have found that the differences between the value g obtained from (49) and (50) and $g(L_c = 30)$ are of order 10^{-5} to 10^{-3} in units of e^2/h for $L_s = [2;16]$. This indicates that the wide band method also works well in 2D.

7.3 In the self-consistent Hartree-Fock approximation

We have then calculated the conductance in 2D with the wide band method in the HF approximation. Figure 7 shows the L_c dependence of the conductance $g(L_c)$ for the wide band system with sample size $L_s = 8$ and $L_s = 16$. The L_c dependence of $g(L_c)$ is qualitatively similar to that in the first order perturbation. We again assume that the influence of the wide band limit is negligible when $L_c = 30$.

In the range $L_c = [21;30]$, the fluctuation of $g(L_c)$ is of order 10^{-3} in units of e^2/h . Assuming that $g(L_c)$ is fluctuating around the asymptotic value g , we can consider the amplitude of the fluctuation as a precision of g in the wide band method.

7.4 L_s dependence of the conductance

Figure 8 shows L_s dependence of the conductance in the first order perturbation and in the HF approximation in 2D. For a reference, the value $N_c e^2/h$ corresponding

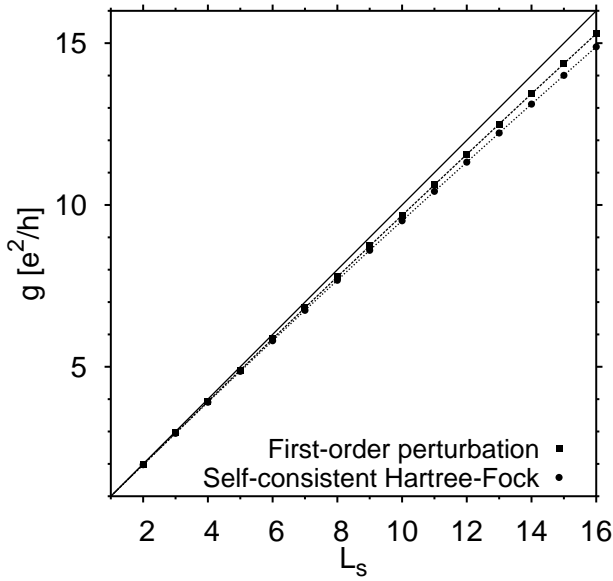


Fig. 8. L_s dependence of the conductance g in 2D in the first-order perturbation and in the HF approximations. We set $K = 0.5$, $\alpha = 0.0$, and $U = 0.5$. For a reference, the conductance corresponding to the perfect transmission $N_c e^2/h$ is also shown. (At $t = 0$, $N_c = L_s$ in the 2D strip imposed fixed boundary conditions in the transverse direction.) The dotted and dashed lines are a guide to the eye only.

to a perfect transmission, with N_c being the number of propagating channels, is also shown. The conductance in the HF approximation tends to be smaller than that in the first order perturbation as it is in 1D

8. Summary and Discussion

We have developed a new numerical method to calculate the Landauer conductance through an interacting electron system at zero temperature in the first order perturbation or in the self-consistent HF approximation. A troublesome numerical integration is avoided by taking a wide band limit. We can remove the artifacts of taking the wide band limit by increasing the length of non-interacting region L_c kept on both sides of the sample. We have applied it to 1D and 2D interacting systems.

The method does not require much CPU time, so it permits us to accumulate many samples in studying interacting disordered systems. Simulation in the presence of disorder is left for future.

The wide band method has an advantage that the dimensionality is not restricted to one. This method can be useful when studying various quantum transport phenomena not only in interacting disordered systems but also in quantum dots, quantum point contacts, quantum nanowires, atomic chains, and so on. It is possible to consider spin degree of freedom. It is also possible to take account of other effects, such as spin-orbit coupling and a magnetic field, by generalizing the wide band method. In the presence of such effects, the effective Hamiltonian might be no longer a complex symmetric matrix. When it is not a complex symmetric matrix, we need to calculate not only the right eigenvectors but also the left eigenvectors.

Acknowledgments

The author thanks Professor Keith Slevin for suggesting him to perform a numerical simulation in the HF approximation, for his critical reading of the manuscript, and for valuable discussions. He would like to thank Professor Jean-Louis Pichard and Dr. Rafael A. Molina for suggesting to put non-interacting regions on the sample, for providing the numerical data of the embedding method used in Fig. 5, and for stimulating discussions. He thanks Professor Tomio Htsuki and Mr. Axel B. Freyn for valuable discussions. He acknowledges the support of the 21st century COE program of Osaka University "Towards a new basic science; depth and synthesis". He is grateful to Research Fellowships of the Japan Society for the Promotion of Science for Young Scientists.

Appendix: Green's functions for semi-infinite leads and some related matrices

In this appendix, the retarded Green's function for semi-infinite leads and some related matrices are shown explicitly. We suppose that the leads are described by the Hamiltonian (3) and coupled with a sample by (4).

First we calculate the retarded Green's function $g^r(\omega)$ for the isolated lead at the left ($x = 0$). In particular, the important elements are those at the surface of the lead, i.e., the elements $g_{0y;0y}^r(\omega)$. The eigenfunctions and eigenvalues of the lead are written as

$$\psi_{k_x, n}(x; y) = \frac{1}{\sqrt{2}} \sin[k_x(x-1)] \phi_n(y); \quad (\text{A } 1)$$

$$E_{k_x, n} = 2t_x \cos k_x + t_y \epsilon_n; \quad (\text{A } 2)$$

where

$$\phi_n(y) = \frac{1}{\sqrt{2(L_y+1)}} \sin k_y^{(n)} y; \quad (\text{A } 3)$$

$$\epsilon_n = 2 \cos k_y^{(n)}; \quad (\text{A } 4)$$

Here $k_x \in [0; \pi]$ is the wave number in the x -direction, and $k_y^{(n)} = n\pi/(L_y+1)$. Using them we have

$$g_{0y;0y}^r(\omega) = \frac{1}{t_x} \sum_{n=1}^{L_y} \frac{\psi_{k_x, n}^*(0; y) \psi_{k_x, n}(0; y)}{E_{k_x, n} - \omega - i0^+}; \quad (\text{A } 5)$$

Here the function $\psi_{k_x, n}(z_n)$ is given by

$$\psi_{k_x, n}(z_n) = \begin{cases} \frac{1}{\sqrt{2}} \left[\frac{z_n}{2} + \frac{z_n^2}{4} - 1 \right] & (z_n < 2) \\ \frac{1}{\sqrt{2}} \left[\frac{z_n}{2} - i \frac{1}{4} \left(\frac{z_n^2}{4} - 1 \right) \right] & (2 < z_n < 2) \\ \frac{1}{\sqrt{2}} \left[\frac{z_n}{2} - \frac{z_n^2}{4} - 1 \right] & (z_n > 2); \end{cases} \quad (\text{A } 6)$$

Similarly, the Green's function for the other lead at the right ($x = L_s + 1$) is obtained as

$$g_{L_s+1y;L_s+1y}^r(\omega) = \frac{1}{t_x} \sum_{n=1}^{L_y} \frac{\psi_{k_x, n}^*(L_s+1; y) \psi_{k_x, n}(L_s+1; y)}{E_{k_x, n} - \omega - i0^+}; \quad (\text{A } 7)$$

A transverse mode n is a propagating mode if $j = \pm n$ and an evanescent mode otherwise. The Fermi wave number $k_F^{(n)}$ ($0 < k_n < \pi$) of the propagating mode n in the x -direction is determined by

$$e^{ik_F^{(n)}} = \frac{z_n}{2} - i \frac{1}{4} \left(\frac{z_n^2}{4} - 1 \right); \quad (\text{A } 8)$$

with $z_n = \tau_n$.

When calculating the Landauer conductance the semi-infinite leads and the sample are coupled by (4). In the Green's function method the effects of the lead are taken account in terms of the self-energy.^{23,38} The retarded self-energy $\epsilon_{xy;x'y^0}^{(r)}$ due to the leads becomes non-zero at the surfaces of the sample, i.e., when $x = x^0 = 1$ or $x = x^0 = L_s$. The non-zero elements are defined by $\epsilon_{1y;1y^0}^{(r)} = t_s^2 g_{0y;0y^0}^r(\epsilon)$ and $\epsilon_{L_s y;L_s y^0}^{(r)} = t_s^2 g_{L_s+1y;L_s+1y^0}^r(\epsilon)$. Using the expression (A 5) we have

$$\epsilon_{xy;x'y^0}^{(r)} = \frac{t_s^2 X^y}{t_n} \sum_{n=1}^{\infty} \gamma_n(\epsilon) \gamma_n(\epsilon^0) \frac{1}{t_n}; \quad (\text{A } 9)$$

where $X = 1$ or L_s .

The L_y L_y matrices $\epsilon^{(L)}$ and $\epsilon^{(R)}$, which appear in the Landauer formula (6), are defined by $\epsilon_{yy^0}^{(L)} = i \epsilon_{1y;1y^0}^r(\epsilon) - i \epsilon_{1y;1y^0}^a(\epsilon)$ and $\epsilon_{yy^0}^{(R)} = i \epsilon_{L_s y;L_s y^0}^r(\epsilon) - i \epsilon_{L_s y;L_s y^0}^a(\epsilon)$. At $\epsilon = \epsilon^0$ we have

$$\epsilon_{yy^0}^{(L;R)} = \frac{2t_s^2 X^0}{t_n} \sum_{n=1}^{\infty} \gamma_n(\epsilon) \gamma_n(\epsilon^0) \sin k_F^{(n)}; \quad (\text{A } 10)$$

Here the summation is taken over propagating modes.

- 1) B. Kramer and A. M. Kohnen: Rep. Prog. Phys. 56 (1993) 1469.
- 2) E. Abraham, S. V. Kravchenko, and M. P. Sarachik: Rev. Mod. Phys. 73 (2001) 251.
- 3) K. M. Itoh, M. Watanabe, Y. Otuka, E. E. Haller, and T. Ohtsuki: J. Phys. Soc. Jpn. 73 (2004) 173.
- 4) H. Fukuyama: J. Phys. Soc. Jpn. 48 (1980) 2169.
- 5) H. Fukuyama: J. Phys. Soc. Jpn. 50 (1981) 3407.
- 6) B. L. Altshuler and A. G. Aronov: in Electron-Electron Interaction in Disordered Conductors, edited by A. L. Efros and M. Pollak (Elsevier, Amsterdam, 1985) Chap. 1, p. 1.
- 7) A. L. Efros and B. I. Shklovskii: J. Phys. C 8 (1975) L49.
- 8) A. L. Efros: J. Phys. C 9 (1976) 2021.
- 9) D. Belitz and T. R. Kirkpatrick: Rev. Mod. Phys. 66 (1994) 261.
- 10) A. H. MacDonald and G. C. Aers: Phys. Rev. B 34 (1986) 2906.
- 11) S.-R. Yang and A. H. MacDonald: Phys. Rev. Lett. 70 (1993) 4110.
- 12) S.-R. Yang, A. H. MacDonald, and B. Huckestein: Phys. Rev. Lett. 74 (1995) 3229.
- 13) F. Epperlein, M. Schreiber, and T. Voja: Phys. Rev. B 56 (1997) 5890.
- 14) G. S. Jeon, S. Wu, M. Y. Choi, and H.-W. Lee: Phys. Rev. B 59 (1999) 2841.
- 15) G. S. Jeon, S. Wu, H.-W. Lee, and M. Y. Choi: Phys. Rev. B 59 (1999) 3033.
- 16) S. Levit and D. Orgad: Phys. Rev. B 60 (1999) 5549.
- 17) M. Lee, G. S. Jeon, and M. Y. Choi: Phys. Rev. B 66 (2002) 075304.
- 18) D. Heidarian and N. Trivedi: Phys. Rev. Lett. 93 (2004) 126401.
- 19) E. Abraham, P. W. Anderson, D. C. Licciardello, and T. V. Ramakrishnan: Phys. Rev. Lett. 42 (1979) 673.
- 20) B. Shapiro: Phil. Mag. B 56 (1987) 1031.
- 21) K. Slevin, P. Markos, and T. Ohtsuki: Phys. Rev. Lett. 86 (2001) 3594.
- 22) K. Slevin, P. Markos, and T. Ohtsuki: Phys. Rev. B 67 (2003) 155106.
- 23) S. Datta: Electronic transport in mesoscopic systems (Cambridge University Press, Cambridge, 1997).
- 24) H. Haug and A.-P. Jauho: Quantum Kinetics in Transport and Optics of Semiconductors (Springer-Verlag, Berlin, 1996).
- 25) T. K. Ng and P. A. Lee: Phys. Rev. Lett. 61 (1988) 1768.
- 26) Y. Meir and N. S. Wingreen: Phys. Rev. Lett. 68 (1992) 2512.
- 27) W. Izumida, O. Sakai, and Y. Shimizu: J. Phys. Soc. Jpn. 66 (1997) 717.
- 28) A. Kawabata: J. Phys. Soc. Jpn. 67 (1998) 2430.
- 29) A. Oguri: Phys. Rev. B 56 (1997) 13422, [Erratum: 58 (1998) 1690].
- 30) A. Oguri: Phys. Rev. B 59 (1999) 12240.
- 31) Y. Tanaka, A. Oguri, and H. Ishii: J. Phys. Soc. Jpn. 71 (2002) 211.
- 32) A. Oguri and A. C. Hewson: J. Phys. Soc. Jpn. 74 (2005) 988.
- 33) O. P. Sushkov: Phys. Rev. B 64 (2001) 155319.
- 34) R. A. Molina, D. Weinmann, R. A. Jalabert, G.-L. Ingold, and J.-L. Pichard: Phys. Rev. B 67 (2003) 235306.
- 35) R. A. Molina, P. Schmitteckert, D. Weinmann, R. A. Jalabert, G.-L. Ingold and J.-L. Pichard: Eur. Phys. J. B 39 (2004) 107.
- 36) V. Meden and U. Schollwöck: Phys. Rev. B 67 (2003) 193303.
- 37) A. L. Fetter and J. D. Walecka: Quantum Theory of Many-Particle Systems (McGraw-Hill, New York, 1971).
- 38) T. Ando: Phys. Rev. B 44 (1991) 8017.
- 39) V. Moldoveanu, A. A. Klea, A. M. Anolescu, and M. Nita: Phys. Rev. B 63 (2001) 045301.
- 40) A. Agarwal and D. Sen: Phys. Rev. B 73 (2006) 045332.
- 41) A.-P. Jauho, N. S. Wingreen, and Y. Meir: Phys. Rev. B 50 (1994) 5528.
- 42) P. M. Morse and H. Feshbach: Methods of theoretical physics (McGraw-Hill, New York, Toronto, London, 1953).
- 43) R. A. Molina, D. Weinmann, and J.-L. Pichard: Europhys. Lett. 67 (2004) 96.
- 44) Y. Asada, J.-L. Pichard, and A. B. Freyn: unpublished.
- 45) Courtesy of R. A. Molina and J.-L. Pichard. Results for larger U are reported in Ref. 43.